

TEM Examination of Precipitation Behaviour of $M_{23}C_6$ and Sigma Phases and Dislocations in SS 310S under Creep Deformation at 800°C

Babak Shalchi Amirkhiz¹, Su Xu¹

¹CanmetMATERIALS, Natural Resources Canada, Hamilton, Canada

Stainless steel 310S is a candidate alloy for fuel cladding of the Canadian Generation IV Supercritical Water-Cooled Reactors (SCWR). In-depth understanding of the creep properties and microstructural evolution of SS 310S during creep is vitally important for the proposed SCWR challenging design conditions, and both are strongly linked to formation, dissolution and coarsening of different precipitates [1]. To the authors' knowledge, a detailed microstructural investigation on crept specimens of SS 310S at 800°C is not available. In this study, precipitation and deformation behaviours of a commercial SS 310S plate (Fe, 24-26wt.% Cr, 19-22% Ni, 2% Mn, 1.5% Si, 0.045% P, 0.03% S, 0.08% C) in the as-received (solution treated), and creep conditions at 800°C were examined using TEM. The creep specimens examined were tested under 30, 50, 70 and 80MPa and the rupture times were 3971, 530, 111, and 59 hours, respectively. All samples were examined using the Tecnai Osiris TEM operating at 200kV.

The as received microstructure of 310S mainly consists of gamma grains with nanometric precipitates of Ti(CN) type. Figure 1 shows general microstructure of ruptured samples under tested conditions. In addition to extensive discrete grain boundary $M_{23}C_6$ carbides, intragranular $M_{23}C_6$ precipitated heterogeneously on Ti(CN) particles (Fig. 2A and C). These carbides are coherent or semi-coherent $Cr_{23}C_6$ as evidenced by electron diffraction analysis (Fig. 2A). The $Cr_{23}C_6$ carbides located in the vicinity of grain boundaries can grow faster as Cr can diffuse through the grain boundaries at a higher rate and transform into σ . The intragranular carbides grow along certain crystallographic orientations (i.e. $\langle 002 \rangle$) and finally transformed to σ . These σ grains are elongated towards $\langle 002 \rangle_\gamma$ (Fig. 2B). Transformation of carbides to σ phase occurred in all creep cases and the areas around large σ grains are free of small precipitates as seen in Fig. 1. When carbides were absent or grew to lose coherency with the gamma matrix or transformed into σ , they did not effectively hinder the movement of dislocations. Consequently, the network of subgrains was disappeared around large σ grains as seen in Fig. 1A, B and C.

Dislocation density (ρ) in crept samples were measured by adjusting a multibeam case in a low index zone and imaging using high angle annular dark-field (HAADF) [2]. A representation of the dislocations in the crept samples is given in Fig. 3. The measured ρ values for samples crept at 80, 70, 50 and 30 MPa were 2.25×10^{14} , 2×10^{14} , 2.67×10^{13} , and $1.36 \times 10^{14} \text{ m}^{-2}$, respectively. While ρ values are close to 10^{14} m^{-2} and generally decreases with decreasing load, the value for the 50MPa sample was one order of magnitude lower as also seen in Fig. 3C. This could be attributed to the ineffectiveness of the carbides in pinning dislocations after growing to a certain size or transforming into σ . In the 30MPa sample a network of dislocations is formed within all gamma grains as seen in Fig. 1D and Fig. 4D. The lower creep resistance of SS 310 compared to common commercial austenitic stainless steels [3] may be due to extensive precipitations observed under creep [4].

References:

[1] T Sourmail, Materials Science and Technology, Vol 17, 1 (2001)

[2] D Rojasa, J Garciab, O Prata, L Agudoc, C Carrascod, G Sauthoffa, AR Kaysser-Pyzallab, Materials Science and Engineering A, **528** (2011), p. 1372.

[3] S. Xu, S.-M. Jin and P. Le Dreff-Kerwin, Proc. PVP 2013, PVP2013-97290.

[4] The authors acknowledge financial support from NRCan program on Energy R&D (PERD)

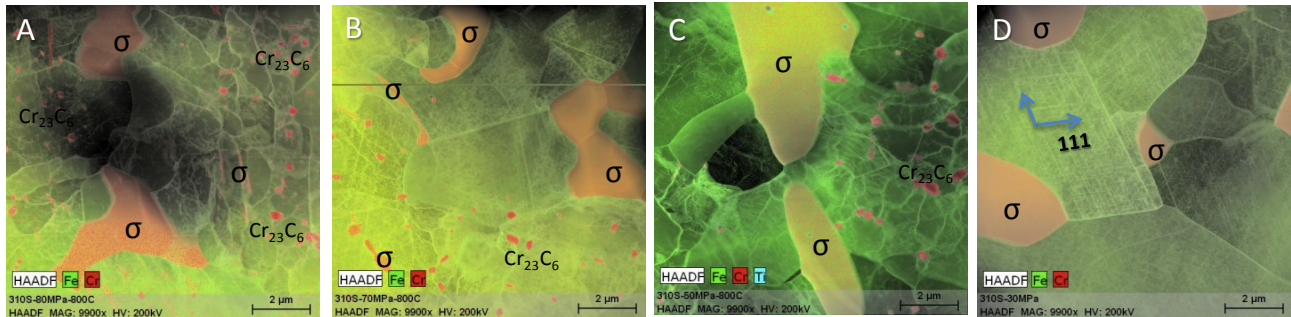


Figure 1. TEM micrographs showing the microstructure of 316S under creep at 800°C in STEM-HAADF images superimposed on EDX Cr elemental map highlighting σ phase and Cr_{23}C_6 carbides in samples crept at (A) 80 MPa, (B) 70 MPa, (C) 50 MPa, and (D) 30 MPa.

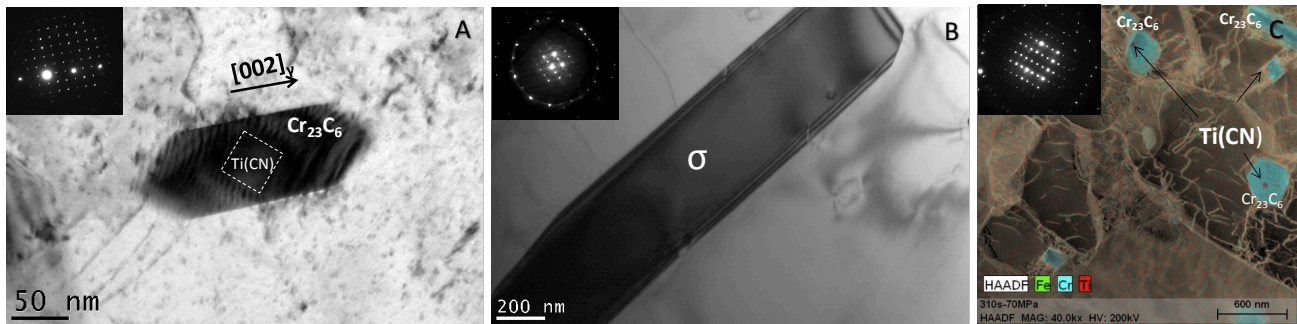


Figure 2. (A) Early growth stage of a Cr_{23}C_6 carbide in the 80 MPa sample, growing towards $[002]_y$, the inset is the corresponding SAD at $\langle 001 \rangle$ zone axis; (B) a Σ precipitate in the 70 MPa sample, the inset is SAD of Σ phase (C) HAADF image overlaid with Fe, Cr and Ti EDS elemental maps showing Cr_{23}C_6 carbides and Ti(CN) particles within them in 70 MPa sample, inset is SAD at from $\langle 121 \rangle$ zone axis of a carbide particle.

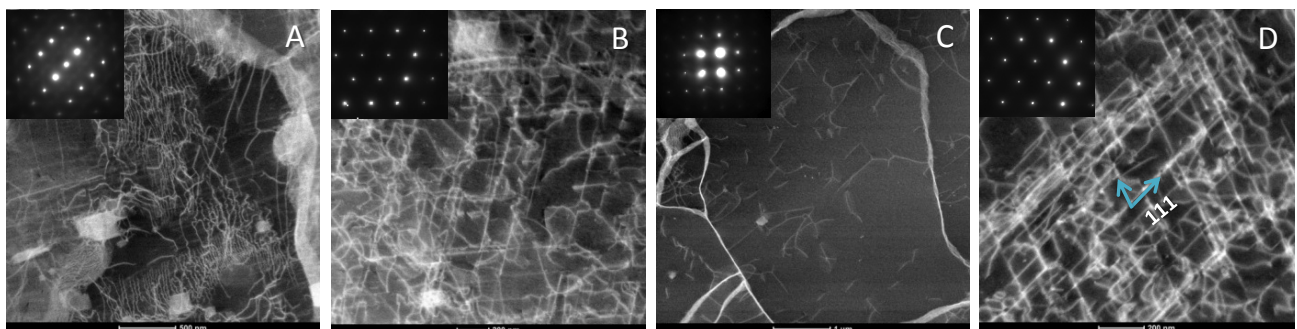


Figure 3. HAADF images representing dislocation density in 310S samples crept for 80, 70, 50 and 30 MPa at 800°C, respectively. Insets show the orientation of the beam regarding the sample, the zone axes are $\langle 122 \rangle$, $\langle 011 \rangle$, $\langle 001 \rangle$ and $\langle 011 \rangle$ respectively from image A to D.